Max-stable processes for modelling extremes observed in space and time

Richard A. Davis[a], Claudia Klüppelberg[b], Christina Steinkohl[c]

[a] *Department of Statistics, Columbia University, New York, United States and Institute for Advanced Study, Technische Universität München, http://www.stat.columbia.edu/~rdavis, Email: rdavis@stat.columbia.edu*

[b] *Center for Mathematical Sciences and Institute for Advanced Study, Technische Universität München, D-85748 Garching, Germany, http://www-m4.ma.tum.de/pers/cklu, Email: cklu@ma.tum.de*

[c] *Center for Mathematical Sciences and Institute for Advanced Study, Technische Universität München, D-85748 Garching, Germany, http://www-m4.ma.tum.de/pers/steinkohl, Email:steinkohl@ma.tum.de*

Abstract

Max-stable processes have proved to be useful for the statistical modelling of spatial extremes. For statistical inference it is often assumed that there is no temporal dependence; i.e., that the observations at spatial locations are independent in time. In a first approach we construct max-stable space-time processes as limits of rescaled pointwise maxima of independent Gaussian processes, where the space-time covariance functions satisfy weak regularity conditions. This leads to so-called Brown-Resnick processes. In a second approach, we extend Smith's storm profile model to a space-time setting. We provide explicit expressions for the bivariate distribution functions, which are equal under appropriate choice of the parameters. We also show how the space-time covariance function of the underlying Gaussian process can be interpreted in terms of the tail dependence function in the limiting max-stable space-time process.

Keywords: Brown-Resnick process, max-stable process, random field in space and time, Smith's storm profile model, spatio-temporal correlation function, Gneiting's class.

Preprint submitted to Elsevier *December 7, 2012*

1. Introduction

The statistical modelling of extremes is an important topic in many applications. Environmental catastrophes like hurricanes, floods and earthquakes can cause substantial damage to structures like bridges, industrial plants and buildings. The basis for an adequate risk analysis in all areas is formed by appropriate stochastic models. Extreme value theory provides the theoretical fundamentals for modelling rare events based on historical data even if there is only a moderate number of extreme observations.

Univariate extreme value theory is well developed and standard introductions can be found in many books, including for example Coles [7], Embrechts, Klüppelberg and Mikosch [19], and Leadbetter, Lindgren and Rootzén [29]. The extension of univariate to multivariate extreme value distributions is presented for instance in Beirlant et al. [4] and de Haan and Ferreira [16]. The process generating the extremes is assumed to be independent, or at least stationary and satisfying some mixing condition (see Leadbetter [28]).S

Max-stable processes are natural extensions of multivariate extreme value distributions to infinite dimensions. Different spectral representations of stationary max-stable processes have been developed for example in de Haan [15], de Haan and Pickands [17], Deheuvels [18], and Schlather [38]. So far, max-stable random fields have mostly been used for the statistical modelling of spatial data, and we call them max-stable spatial fields. Examples include Coles [6] and Coles and Tawn [8], who model extremal rainfall fields using max-stable processes. Another application to rainfall data can be found in Padoan, Ribatet and Sisson [34], who also describe a practicable pairwise likelihood estimation procedure. This method as well as a new semiparametric estimation method is applied in Davis, Klüppelberg and Steinkohl [11] to radar rainfall data. An interesting application to wind gusts is shown in Coles and Walshaw [9], who use max-stable processes to model the angular dependence for wind speed directions.

Different approaches for constructing max-stable processes have been introduced, and we mention two examples here, which we will apply to the space-time setting. In some cases the approaches can lead to the same finite-dimensional distribution functions.

The idea of constructing max-stable spatial fields as limits of normalized and scaled pointwise maxima of Gaussian random fields was introduced in Kabluchko, Schlather and de Haan [27], who construct max-stable spatial fields associated with a class of variograms. The limit field in this approach has the same finite dimensional distributions as the so-called Brown-Resnick process (see Brown and Resnick [5] or Kabluchko et al. [27]).

In an earlier paper Smith [42] introduced also a max-stable process, which became known as the storm profile model. The different variables in the construction have an interpretation as components in a storm, including the shape and the intensity. The process is based on points from a Poisson random measure $\{(\xi_j, \boldsymbol{u}_j),\ j \geq 1\}$ together with a kernel function f, which in particular can be a centered Gaussian density. The max-stable process then arises from $\eta(\boldsymbol{y}) = \max_{j\geq 1} \xi_j f(\boldsymbol{y}; \boldsymbol{u}_j)$.

In real world applications, measurements are typically taken at various locations, sometimes on a grid, and at regularly spaced time intervals. For statistical inference, it is then often assumed that the measurements are independent in time. We mention two approaches proposed in the literature concerning the analysis and quantification of the extremal behaviour of processes observed both in space and time. One idea can be found in Davis and Mikosch [13], who study the extremal properties of a moving average process of spatial fields, where the coefficients and the white-noise process depend on space and time. Sang and Gelfand [37] propose a hierarchical modelling procedure, where on a latent stage spatio-temporal dependence is included via the parameters of the generalized extreme value distribution. Extremes of space-time Gaussian processes have been studied in Kabluchko [26]. He analyses processes of the form $\sup_{t'\in[0,tn]} Z(s_n \boldsymbol{s}, t')$ for some suitably chosen space-time Gaussian process and shows that the finite dimensional distributions of a properly scaled version converge to those of a Brown-Resnick process.

For an extension of the approach of Kabluchko et al. [27] to a space-time model we need an underlying spatio-temporal correlation model for the Gaussian process, which satisfies a certain regularity condition at 0. This condition, taken from a well-known result by Hüsler and Reiss [25], assumes that a rescaled version of the correlation function $\rho(\boldsymbol{h}, u)$ for the space-lag $\boldsymbol{h}$ and the temporal lag u satisfies $(\log n)(1 - \rho(s_n\boldsymbol{h}, t_n u)) \to \delta(\boldsymbol{h}, u)$ as $n \to \infty$ for scaling sequences s_n and t_n. We establish an explicit connection between the limit $\delta(\boldsymbol{h}, u)$ and the tail dependence coefficient for two different locations at two different time points.

Recently, the development of covariance models in space and time has received much attention and there is now a large literature available for the construction of a wide-range of spatio-temporal covariance functions. Examples can be found in Cressie and Huang [10], Gneiting [24], Ma [32, 30], and Schlather [39]. Within this context, we generalize an assumption on correlation functions for the analysis of extremes from stationary Gaussian processes (see for instance Leadbetter et al. [29], Chapter 12), which is a sufficient condition for the limit assumption described above. We show how Gneiting's class of nonseparable and isotropic covariance functions [24] fits into this framework.

In addition, we examine spatial anisotropic correlation functions, which allow for directional dependence in the spatial components. An easy way to introduce anisotropy in a model is to use geometric anisotropy. For a detailed introduction, we refer to Wackernagel [43], Chapter 9. Using this concept in the underlying correlation function, we can model anisotropy in the corresponding max-stable spatial field. Furthermore, we revisit a more elaborate way of constructing anisotropic correlation models based on Bernstein functions introduced by Porcu, Gregori and Mateu [36], called the Bernstein class.

Our paper is organized as follows. The two approaches for the construction of space-time max-stable processes are described in Section 2. The max-stable process, which is based on the maximum of rescaled and transformed replications of Gaussian space-time process is presented in Section 2.1, while

Smith's storm profile model is extended to a space-time setting in Section 2.2. In Section 3, we show how Pickands dependence function and the tail dependence coefficient relate to the correlation model used in the underlying Gaussian process. Further correlation models are discussed in Section 4 and simulations based on a set of different parameters are visualized. Section 4.2 analyzes anisotropic correlation functions, where one can see directional movements in the storm profile model.

2. Extension of max-stable spatial fields to the space-time setting

Max-stable processes form the natural extension of multivariate extreme value distributions to infinite dimensions. In the literature, different approaches for establishing space-time max-stable processes have been considered. In this section, we discuss two approaches for constructing such processes and apply the concepts to a space-time setting. In Section 2.1 we describe the construction introduced in Kabluchko, Schlather and de Haan [27] based on a limit of pointwise maxima from an array of independent Gaussian processes. Furthermore, we use the approach introduced in de Haan [15] and interpreted by Smith [42] as the storm profile model in a space-time setting in Section 2.2.

2.1. Max-stable processes based on space-time correlation functions

Before presenting the construction of a max-stable space-time process, we begin with the definition of the Brown-Resnick space-time process with Fréchet marginals (see Brown and Resnick [5] or Schlather [38]). Let $\{\xi_j, j \geq 1\}$ denote points of a Poisson random measure on $[0, \infty)$ with intensity measure $\xi^{-2} d\xi$ and let $Y_j(\boldsymbol{s}, t),\ j \geq 1$ be independent replications of some space-time process $\left\{Y(\boldsymbol{s}, t), (\boldsymbol{s}, t) \in \mathbb{R}^d \times [0, \infty)\right\}$ with $\mathbb{E}(Y(\boldsymbol{s}, t)) < \infty$, and $Y(\boldsymbol{s}, t) \geq 0$ *a.s.*, which are also independent of ξ_j. The process

$$\eta(\boldsymbol{s}, t) = \bigvee_{j=1}^{\infty} \{\xi_j Y_j(\boldsymbol{s}, t)\}, \quad (\boldsymbol{s}, t) \in \mathbb{R}^d \times [0, \infty), \tag{2.1}$$

where $\bigvee_{j=1}^{\infty} x_j$ denotes the maximum operator $\max\{x_j, j \geq 1\}$, is a max-stable process with Fréchet marginals and often refered to as the Brown-Resnick process (see Kabluchko et al. [27]). The finite-dimensional distributions can be calculated using a point process argument as done in de Haan [15]. For example, if $(\boldsymbol{s}_1, t_1), \ldots, (\boldsymbol{s}_K, t_K)$ are distinct space-time locations (duplicates in the space or the time components are allowed), then

$$\begin{aligned}
&P(\eta(\boldsymbol{s}_1, t_1) \leq y_1, \ldots, \eta(\boldsymbol{s}_K, t_K) \leq y_K) \\
&= P\left(\xi_j \bigvee_{k=1}^{K} \frac{Y_j(\boldsymbol{s}_k, t_k)}{y_k} \leq 1 \text{ for all } j \geq 1\right) \\
&= P\left(N(A) = 0\right) = \exp\left\{-\mathbb{E}\left(\bigvee_{k=1}^{K} \frac{Y(\boldsymbol{s}_k, t_k)}{y_k}\right)\right\}, \qquad (2.2)
\end{aligned}$$

where $A = \{(u, v); uv > 1\}$ and N is the Poisson random measure with points

$$\left\{\left(\xi_j, \bigvee_{k=1}^{K} \frac{Y_j(\boldsymbol{s}_k, t_k)}{y_k}\right), \quad j \geq 1\right\}.$$

As we will see below, the Brown-Resnick process is the limit of a sequence of pointwise maxima of independent Gaussian space-time processes. In the following, let $\{Z(\boldsymbol{s}, t)\}$ denote a Gaussian space-time process on $\mathbb{R}^d \times [0, \infty)$ with covariance function given by

$$\tilde{C}(\boldsymbol{s}_1, t_1; \boldsymbol{s}_2, t_2) = \mathbb{C}ov\left(Z(\boldsymbol{s}_1, t_1), Z(\boldsymbol{s}_2, t_2)\right),$$

for two locations $\boldsymbol{s}_1, \boldsymbol{s}_2 \in \mathbb{R}^d$ and time points $t_1, t_2 \in [0, \infty)$. We assume stationarity in space and time, so that we can write

$$\tilde{C}(\boldsymbol{s}_1, t_1; \boldsymbol{s}_2, t_2) = C(\boldsymbol{s}_1 - \boldsymbol{s}_2, t_1 - t_2) = C(\boldsymbol{h}, u),$$

where $\boldsymbol{h} = \boldsymbol{s}_1 - \boldsymbol{s}_2$ and $u = t_1 - t_2$. Furthermore, let $\rho(\boldsymbol{h}, u) = C(\boldsymbol{h}, u)/C(\boldsymbol{0}, 0)$ denote the corresponding correlation function. We will assume smoothness conditions on $\rho(\cdot, \cdot)$ near $(\boldsymbol{0}, 0)$. This assumption is natural in the context of space-time processes, since it basically relates to the smoothness of the underlying Gaussian space-time process.

Assumption 2.1. *There exist non-negative sequences of constants* $s_n \to 0,\ t_n \to 0$ *as* $n \to \infty$ *and a non-negative function* δ *such that*

$$(\log n)(1-\rho(s_n(\boldsymbol{s}_1-\boldsymbol{s}_2), t_n(t_1-t_2))) \to \delta(\boldsymbol{s}_1-\boldsymbol{s}_2, t_1-t_2) \in (0,\infty), \quad n \to \infty,$$

for all $(\boldsymbol{s}_1, t_1) \neq (\boldsymbol{s}_2, t_2),\ (\boldsymbol{s}_1, t_1), (\boldsymbol{s}_2, t_2) \in \mathbb{R}^d \times [0,\infty)$.

Examples of such correlation functions are given in Section 4. If $(\boldsymbol{s}_1, t_1) = (\boldsymbol{s}_2, t_2)$, it follows that the correlation function equals one, $\rho(\mathbf{0}, 0) = 1$, which directly leads to $\delta(\mathbf{0}, 0) = 0$. The following theorem regarding limits of finite-dimensional distributions stems from Theorem 1 in Hüsler and Reiss [25]. Throughout we denote by $C(\mathbb{R}^d \times [0,\infty))$ the space of continuous functions on $\mathbb{R}^d \times [0,\infty)$, where convergence is defined as uniform convergence on compact subsets of $\mathbb{R}^d \times [0,\infty)$.

Theorem 2.2. *Let* $Z_j(\boldsymbol{s}, t),\ j = 1, 2, \ldots$ *be independent replications from a stationary Gaussian space-time process with mean* 0*, variance* 1 *and correlation model* ρ *satisfying Assumption 2.1 with limit function* δ*. Assume there exists a metric* D *on* $\mathbb{R}^d \times [0,\infty)$ *such that*

$$\delta(\boldsymbol{s}_1 - \boldsymbol{s}_2, t_1 - t_2) \leq (D((\boldsymbol{s}_1, t_1), (\boldsymbol{s}_2, t_2)))^2 \tag{2.3}$$

and

$$\eta_n(\boldsymbol{s}, t) = \frac{1}{n} \bigvee_{j=1}^{n} -\frac{1}{\log\left(\Phi(Z_j(s_n \boldsymbol{s}, t_n t))\right)}, \quad (\boldsymbol{s}, t) \in \mathbb{R}^d \times [0,\infty), \tag{2.4}$$

where $\Phi(\cdot)$ *denotes the standard normal distribution function, and* (s_n) *and* (t_n) *are the scaling sequences from Assumption 2.1. Then,*

$$\eta_n(\boldsymbol{s}, t) \xrightarrow{\mathcal{L}} \eta(\boldsymbol{s}, t), \quad n \to \infty, \tag{2.5}$$

where $\xrightarrow{\mathcal{L}}$ *denotes weak convergence in* $C(\mathbb{R}^d \times [0,\infty))$ *and* $\left\{\eta(\boldsymbol{s}, t), (\boldsymbol{s}, t) \in \mathbb{R}^d \times [0,\infty)\right\}$ *is a Brown-Resnick space-time process. The bi-*

variate distribution functions of $\eta(\boldsymbol{s}, t)$ are given by

$$F(y_1, y_2) = \exp\left\{-\frac{1}{y_1}\Phi\left(\frac{\log\frac{y_2}{y_1}}{2\sqrt{\delta(\boldsymbol{h}, u)}} + \sqrt{\delta(\boldsymbol{h}, u)}\right) - \frac{1}{y_2}\Phi\left(\frac{\log\frac{y_1}{y_2}}{2\sqrt{\delta(\boldsymbol{h}, u)}} + \sqrt{\delta(\boldsymbol{h}, u)}\right)\right\}. \tag{2.6}$$

Remark 2.3. Condition (2.3) is sufficient to prove tightness of the sequence $(\eta_n)_{n\in\mathbb{N}}$ in $C(\mathbb{R}^d \times [0, \infty))$. As shown in the proof of Theorem 17 in Kabluchko et al. [27] the limit process η is a Brown-Resnick process as in (2.1) with Y given by

$$\exp\{W(\boldsymbol{s}, t) - \delta(\boldsymbol{s}, t)\}, \ (\boldsymbol{s}, t) \in \mathbb{R}^d \times [0, \infty),$$

where $\{W(\boldsymbol{s}, t), \ (\boldsymbol{s}, t) \in \mathbb{R}^d \times [0, \infty)\}$ is a Gaussian process with mean 0 and covariance function

$$\mathbb{C}ov(W(\boldsymbol{s}_1, t_1), W(\boldsymbol{s}_2, t_2)) = \delta(\boldsymbol{s}_1, t_1) + \delta(\boldsymbol{s}_2, t_2) - \delta(\boldsymbol{s}_1 - \boldsymbol{s}_2, t_1 - t_2). \tag{2.7}$$

In particular, δ is a variogram leading to a valid covariance function in (2.7). □

Proof. Although this proof is similar to the one given in Kabluchko et al. [27], we provide a sketch of the argument for completeness. We start with the bivariate distributions. From classical extreme value theory (see for example Embrechts, Klüppelberg and Mikosch [19], Example 3.3.29), for

$$b_n = \sqrt{2\log n} - \frac{\log\log n + \log(4\pi)}{2\sqrt{2\log n}} \tag{2.8}$$

we have

$$\lim_{n\to\infty} \Phi^n\left(b_n + \frac{\log(y)}{b_n}\right) = e^{-1/y}, \quad y > 0.$$

By using the standard arguments as in [19], it follows that

$$\Phi^{-1}\left(e^{-1/ny}\right) \sim \frac{\log y}{b_n} + b_n, \quad n \to \infty, \tag{2.9}$$

where $\sim$ denotes asymptotic equivalence, i.e. two sequences are asymptotically equivalent, $a_n \sim b_n$, if $a_n/b_n \to 1$ as $n \to \infty$. By applying (2.9) and Theorem 1 in Hüsler and Reiss [25] to the random variables $\eta_n(\boldsymbol{s}_1, t_1)$ and $\eta_n(\boldsymbol{s}_2, t_2)$ for fixed different $(\boldsymbol{s}_1, t_1), (\boldsymbol{s}_2, t_2) \in \mathbb{R}^d \times [0, \infty)$, we obtain for $y_1, y_2 > 0$

$$
\begin{aligned}
&P(\eta_n(\boldsymbol{s}_1, t_1) \le y_1, \eta_n(\boldsymbol{s}_2, t_2) \le y_2) \\
&= P\left(\bigvee_{j=1}^{n} -\frac{1}{\log(\Phi(Z_j(s_n \boldsymbol{s}_1, t_n t_1)))} \le n y_1, \bigvee_{j=1}^{n} -\frac{1}{\log(\Phi(Z_j(\boldsymbol{s}_2, t_n t_2)))} \le n y_2 \right) \\
&= P\left(\bigvee_{j=1}^{n} Z_j(s_n \boldsymbol{s}_1, t_n t_1) \le \Phi^{-1}\left(e^{-1/(n y_1)}\right), \bigvee_{j=1}^{n} Z_j(\boldsymbol{s}_2, t_n t_2) \le \Phi^{-1}\left(e^{-1/(n y_2)}\right) \right) \\
&\sim P^n\left(Z_1(s_n \boldsymbol{s}_1, t_n t_1) \le \frac{\log(y_1)}{b_n} + b_n, Z_1(s_n \boldsymbol{s}_2, t_n t_2) \le \frac{\log(y_2)}{b_n} + b_n \right) \\
&\sim \exp\left\{ -\frac{1}{y_1} - \frac{1}{y_2} \right. \\
&\qquad \left. + nP\left(Z_1(s_n \boldsymbol{s}_1, t_n t_1) > \frac{\log(y_1)}{b_n} + b_n, Z_1(s_n \boldsymbol{s}_2, t_n t_2) > \frac{\log(y_2)}{b_n} + b_n \right) \right\}.
\end{aligned}
$$

The pair $(Z_1(s_n \boldsymbol{s}_1, t_n t_1), Z_2(s_n \boldsymbol{s}_2, t_n t_2))$ is bivariate normally distributed with mean $\mathbf{0}$ and covariance matrix given by $\rho(s_n(\boldsymbol{s}_1 - \boldsymbol{s}_2), t_n(t_1 - t_2))$. Using the properties of the conditional normal distribution and Assumption 2.1, it can be shown that the last expression converges to (2.6). Similarly to the procedure above, the higher finite-dimensional limit distributions can be calculated by using Theorem 2 in Hüsler and Reiss [25].

It remains to show that the sequence $(\eta_n)_{n \in \mathbb{N}}$ is tight in $C(\mathbb{R}^d \times [0, \infty))$. Recall that for fixed $\boldsymbol{s} \in \mathbb{R}^d$ and $t \in [0, \infty)$ and $n \in \mathbb{N}$ the process $\eta_n(\boldsymbol{s}, t)$ is (in probability) asymptotically equivalent to $\bigvee_{j=1}^n b_n(Z_j(s_n \boldsymbol{s}, t_n t) - b_n) = \bigvee_{j=1}^n Y_{j,n}(\boldsymbol{s}, t)$, where b_n is defined in (2.8). To show that $(\eta_n)_{n \in \mathbb{N}}$ is tight in $C(\mathbb{R}^d \times [0, \infty))$, Kabluchko et al. [27] show that the conditional family of processes $\left\{ Y_n^{\omega}(\boldsymbol{s}, t),\ (\boldsymbol{s}, t) \in \mathbb{R}^d \times [0, \infty) \right\}$, defined for $\omega \in [-c, c]$ and $n \in \mathbb{N}$

as follows:

$$
\begin{aligned}
&Y_n^\omega(\boldsymbol{s},t) = (Y_n(\boldsymbol{s},t)-\omega) \mid \{Y_n(\mathbf{0},0)=\omega\},\\
&= (b_n(Z(s_n\boldsymbol{s},t_nt)-b_n)-\omega) \mid \{b_n(Z(\mathbf{0},0)-b_n)=\omega\}, \quad \omega\in[-c,c],\ n\in\mathbb{N},
\end{aligned}
$$

is tight in $C(K)$, where K is any compact subset of $\mathbb{R}^d\times[0,\infty)$. This is achieved by calculating an upper bound for the variance of the distance between the process at two different spatio-temporal locations, which in our case is given by assumption (2.3). That is, for large n,

$$
\begin{aligned}
\mathbb{V}ar(Y_n^\omega(\boldsymbol{s}_1,t_1)-Y_n^\omega(\boldsymbol{s}_2,t_2)) &\le 2b_n^2(1-\rho(s_n(\boldsymbol{s}_1-\boldsymbol{s}_2),t_n(t_1-t_2)))\\
&\le 2B\delta(\boldsymbol{s}_1-\boldsymbol{s}_2,t_1-t_2)\le 2BD((\boldsymbol{s}_1,t_1),(\boldsymbol{s}_1,t_2))^2,
\end{aligned}
$$

for some constant $B>0$. The remainder of the proof follows analogously to the proof in [27]. □

Remark 2.4. Kabluchko [26] studies the limit behavior of rescaled space-time processes of the form

$$
\sup_{t'\in[0,tn]} Z(s_n\boldsymbol{s},t')
$$

and shows that a rescaled version converges in the sense of finite-dimensional distributions to a Brown-Resnick space-time process. The assumptions on the covariance function in the underlying Gaussian space-time process are similar to those we use in Section 4. The approach differs from ours in the sense that we analyse the pointwise maxima of independent replications of some space-time process, rather than the supremum over time of a single process. □

Remark 2.5. In applications, the marginal distributions are often fitted by a generalized extreme value distribution and are then transformed to standard Fréchet. Sometimes it may be useful to think about other marginal distributions, such as the Gumbel or Weibull. In order to use Gumbel marginals, we need to define

$$
\eta_n(\boldsymbol{s},t) = \bigvee_{j=1}^{n} -\log\left(-\log\left(\Phi\left(Z_j(s_n\boldsymbol{s},t_nt)\right)\right)\right)-\log(n), \tag{2.10}
$$

and obtain the bivariate distribution function in (2.6) with $1/y_1$ and $1/y_2$ replaced by e^{-y_1} and e^{-y_2}, respectively. If we want to use Weibull marginals in our model, we define

$$\eta_n(\boldsymbol{s},t) = n \bigvee_{j=1}^{n} \log\left(\Phi\left(Z_j(s_n\boldsymbol{s}, t_n t)\right)\right), \tag{2.11}$$

leading to the same bivariate distribution function as in (2.6), but with $1/y_1$ and $1/y_2$ replaced by y_1 and y_2, respectively. □

2.2. Extension of Smith's storm profile model

In this section, we extend the max-stable spatial process, first introduced in de Haan [15], to a space-time setting. The spatial process was interpreted by Smith [42] as a model for storms, where each component can be interpreted as an element of a storm, like its intensity or center. In later papers, including for instance Schlather and Tawn [40] this process is called the storm profile model. We extend the concept to a space-time setting, where extremes are observed at certain locations through time. For simplicity of presentation we assume without loss of generality that $\mathbb{R}^2$ is the space domain. Assume that we have a domain for point processes of storm centres $Z \subset \mathbb{R}^2$ and a time domain $X \subset [0,\infty)$, for which the storm is strongest at its centres. Further, let $\{(\xi_j, \boldsymbol{z}_j, x_j), j \geq 1\}$ denote the points of a Poisson random measure on $(0,\infty) \times Z \times X$ with intensity measure $\xi^{-2}d\xi \times \lambda_2(d\boldsymbol{z}) \times \lambda_1(dx)$, where λ_d denotes Lebesgue measure on $\mathbb{R}^d$ for $d = 1, 2$. Each ξ_j represents the intensity of storm j. Moreover, let $f(\boldsymbol{z}, x; \boldsymbol{s}, t)$ for $(\boldsymbol{z}, x) \in Z\times X$ and $(\boldsymbol{s}, t) \in \mathbb{R}^d\times[0,\infty)$ be a non-negative function with

$$\int_{Z\times X} f(\boldsymbol{z}, x; \boldsymbol{s}, t)\lambda_2(d\boldsymbol{z})\lambda_1(dx) = 1, \quad (\boldsymbol{s}, t) \in \mathbb{R}^2 \times [0,\infty).$$

The function f represents the shape of the storm. Define

$$\eta(\boldsymbol{s}, t) = \bigvee_{j\geq 1} \left\{\xi_j f(\boldsymbol{z}_j, x_j; \boldsymbol{s}, t)\right\}, \quad (\boldsymbol{s}, t) \in \mathbb{R}^2 \times [0,\infty). \tag{2.12}$$

The product $\xi_j f(\boldsymbol{z}_j, x_j; \boldsymbol{s}, t)$ can be interpreted as the wind speed at location $\boldsymbol{s}$ and time point t from storm j with intensity ξ_j, spatial location of the center $\boldsymbol{z}_j$ and maximum wind speed at this centre at time x_j. The joint distribution function of $(\eta(\boldsymbol{s}_1, t_1), \ldots, \eta(\boldsymbol{s}_K, t_K))$, defined for fixed $(\boldsymbol{s}_1, t_1), \ldots, (\boldsymbol{s}_K, t_K) \in \mathbb{R}^d \times [0, \infty)$ and $y_1, \ldots, y_K > 0$, is given through the spectral representation calculated in de Haan [15] as

$$F(y_1, \ldots, y_K) = \exp\left\{ - \int\limits_{Z \times X} \bigvee_{k=1}^{K} \frac{f(\boldsymbol{z}, x; \boldsymbol{s}_k, t_k)}{y_k} \lambda_2(d\boldsymbol{z})\lambda_1(dx) \right\} \quad (2.13)$$

To connect the storm model with the Brown-Resnick process from Theorem 2.2, we assume a trivariate Gaussian density for the function f with mean $(\boldsymbol{z}, x)$ and covariance matrix $\tilde{\Sigma}$, i.e.

$$f(\boldsymbol{z}, x; \boldsymbol{s}, t) = f_0(\boldsymbol{z} - \boldsymbol{s}, x - t),$$

where f_0 is a Gaussian density with mean $\mathbf{0}$ and covariance matrix $\tilde{\Sigma}$. We assume that the spatial dependence is modelled through the matrix Σ and the temporal dependence is given through σ_3^2, leading to the covariance matrix

$$\tilde{\Sigma} = \begin{pmatrix} \Sigma & \mathbf{0} \\ \mathbf{0} & \sigma_3^2 \end{pmatrix} = \begin{pmatrix} \sigma_1^2 & \sigma_{12} & 0 \\ \sigma_{12} & \sigma_2^2 & 0 \\ 0 & 0 & \sigma_3^2 \end{pmatrix}. \quad (2.14)$$

In the following theorem, we calculate a closed form of the bivariate distribution function resulting from the setting defined above. The derivation of the bivariate distribution function in a purely spatial setting can be found in Padoan, Ribatet and Sisson [34] and we stick closely to their notation. The idea of the proof is widely known and, for completeness, details are given in Appendix Appendix A.

Theorem 2.6. *With the setting defined above, the max-stable space-time process*

$$\eta(\boldsymbol{s}, t) = \bigvee_{j \geq 1} \left\{ \xi_j f_0(\boldsymbol{z}_j - \boldsymbol{s}; x_j - t) \right\}, \quad (\boldsymbol{s}, t) \in \mathbb{R}^2 \times [0, \infty), \quad (2.15)$$

has the bivariate distribution function given by

$$\begin{aligned} F(y_1, y_2) &= P(\eta(\boldsymbol{s}_1, t_1) \le y_1, \eta(\boldsymbol{s}_2, t_2) \le y_2) \\ &= \exp\left\{ -\frac{1}{y_1}\Phi\left(\frac{2\sigma_3^2 \log(y_2/y_1) + \sigma_3^2 a(\boldsymbol{h})^2 + u^2}{2\sigma_3\sqrt{\sigma_3^2 a(\boldsymbol{h})^2 + u^2}} \right) \right. \\ &\quad \left. -\frac{1}{y_2}\Phi\left(\frac{2\sigma_3^2 \log(y_1/y_2) + \sigma_3^2 a(\boldsymbol{h})^2 + u^2}{2\sigma_3\sqrt{\sigma_3^2 a(\boldsymbol{h})^2 + u^2}} \right) \right\}, \end{aligned} \tag{2.16}$$

where $\boldsymbol{h} = \boldsymbol{s}_1 - \boldsymbol{s}_2$ *is the space lag,* $u = t_1 - t_2$ *is the time lag and* $a(\boldsymbol{h}) = (\boldsymbol{h}^T \Sigma^{-1} \boldsymbol{h})^{1/2}$.

Note, that if the time lag u equals zero, the formula reduces to

$$F(y_1, y_2) = \exp\left\{ -\frac{1}{y_1}\Phi\left(\frac{a(\boldsymbol{h})}{2} + \frac{\log(y_2/y_1)}{a(\boldsymbol{h})} \right) - \frac{1}{y_2}\Phi\left(\frac{a(\boldsymbol{h})}{2} + \frac{\log(y_1/y_2)}{a(\boldsymbol{h})} \right) \right\},$$

which is the bivariate distribution of the max-stable spatial field as calculated in Padoan, Ribatet and Sisson [34]. If the space lag $\boldsymbol{h}$ is zero, the bivariate distribution function is given by

$$\begin{aligned} &F(y_1, y_2) \\ &= \exp\left\{ -\frac{1}{y_1}\Phi\left(\frac{1}{u}\left(\log(\frac{y_2}{y_1} + \frac{u^2}{2\sigma_3^2} \right) \right) - \frac{1}{y_2}\Phi\left(\frac{1}{u}\left(\log(\frac{y_1}{y_2}) + \frac{u^2}{2\sigma_3^2} \right) \right) \right\}. \end{aligned}$$

By comparing the bivariate distributions of Smith's storm profile model with those in (2.6), we note that the distribution functions are the same, provided that

$$\delta(\boldsymbol{h}, u) = \frac{1}{4} a(\boldsymbol{h})^2 + \frac{1}{\sigma_3^2} u^2, \quad \boldsymbol{h} \in \mathbb{R}^2, u \in \mathbb{R}. \tag{2.17}$$

3. Pickands dependence function and tail dependence coefficient

The Pickands dependence function (Pickands [35]) is one measure of tail dependence and is related to the so-called exponent measure. A general introduction to exponent measures and Pickands dependence function can be found in Beirlant et al. [4]. In particular, the bivariate distributions of the max-stable process can be expressed with the exponent measure V,

$$P(\eta(\boldsymbol{s}_1, t_1) \leq y_1, \eta(\boldsymbol{s}_2, t_2) \leq y_2) = \exp\left\{-V(y_1, y_2; \delta(\boldsymbol{s}_1 - \boldsymbol{s}_2, t_1 - t_2))\right\},$$

where in our case V is given by the bivariate distribution function (2.6) as

$$\begin{aligned} &V(y_1, y_2; \delta(\boldsymbol{h}, u)) \\ &= \frac{1}{y_1}\Phi\left(\frac{\log\left(\frac{y_2}{y_1}\right)}{2\sqrt{\delta(\boldsymbol{h}, u)}} + \sqrt{\delta(\boldsymbol{h}, u)}\right) + \frac{1}{y_2}\Phi\left(\frac{\log\left(\frac{y_1}{y_2}\right)}{2\sqrt{\delta(\boldsymbol{h}, u)}} + \sqrt{\delta(\boldsymbol{h}, u)}\right) \end{aligned}$$

and depends on the space and time lags $\boldsymbol{h}$ and u.

The Pickands dependence function is now defined through

$$\exp\left\{-V(y_1, y_2, \delta(\boldsymbol{h}, u))\right\} = \exp\left\{-\left(\frac{1}{y_1} + \frac{1}{y_2}\right) A\left(\frac{y_1}{y_1 + y_2}\right)\right\}.$$

Setting $\lambda = y_1/(y_1 + y_2)$, hence $1 - \lambda = y_2/(y_1 + y_2)$, we obtain

$$\begin{aligned} &A(\lambda; \delta(\boldsymbol{h}, u)) = \lambda(1-\lambda)V(\lambda, 1-\lambda; \delta(\boldsymbol{h}, u)) \\ &= \lambda\Phi\left(\frac{\log\frac{\lambda}{1-\lambda}}{2\sqrt{\delta(\boldsymbol{h}, u)}} + \sqrt{\delta(\boldsymbol{h}, u)}\right) + (1-\lambda)\Phi\left(\frac{\log\frac{1-\lambda}{\lambda}}{2\sqrt{\delta(\boldsymbol{h}, u)}} + \sqrt{\delta(\boldsymbol{h}, u)}\right). \end{aligned}$$

A useful summary measure for extremal dependence is the tail-dependence coefficient, which goes back to Geffroy [22, 23] and Sibuya [41]. It is defined by

$$\chi = \lim_{x\to\infty} P\left(\eta(\boldsymbol{s}_1, t_1) > F^{\leftarrow}_{\eta(\boldsymbol{s}_1, t_1)}(x) \mid \eta(\boldsymbol{s}_2, t_2) > F^{\leftarrow}_{\eta(\boldsymbol{s}_2, t_2)}(x)\right),$$

where $F^{\leftarrow}_{\eta(\boldsymbol{s},t)}$ is the generalized inverse of the marginal distribution for fixed location $\boldsymbol{s} \in S$ and time point $t \in T$. For our model this leads to

$$\chi(\boldsymbol{h}, u) = 2(1 - \Phi(\sqrt{\delta(\boldsymbol{h}, u)})). \tag{3.1}$$

The tail dependence coefficient is a special case of the extremogram introduced in Davis and Mikosch [14], Section 1.4, with the sets A and B defined as $(1, \infty)$; this was also considered in Fasen, Klüppelberg and Schlather [20].

The two cases $\chi(\boldsymbol{h}, u) = 0$ and $\chi(\boldsymbol{h}, u) = 1$ correspond to the boundary cases of asymptotic independence and complete dependence. Thus, if $\delta(\boldsymbol{h}, u) \to 0$, the marginal components in the bivariate case are completely dependent and if $\delta(\boldsymbol{h}, u) \to \infty$, the components become independent. In the following section, we examine the relationship between the underlying correlation function and the tail dependence coefficient.

4. Possible correlation functions for the underlying Gaussian process

Provided the correlation function of the underlying Gaussian process is sufficiently smooth near $(\mathbf{0}, 0)$, Assumption 2.1 holds for some positive sequences s_n and t_n. One such condition is given below. Throughout this section let $\boldsymbol{h} = \boldsymbol{s}_1 - \boldsymbol{s}_2$ denote the space lag and $u = t_1 - t_2$ the time lag.

Assumption 4.1. *Assume that the correlation function allows for the following expansion*

$$\rho(\boldsymbol{h}, u) = 1 - C_1 \|\boldsymbol{h}\|^{\alpha_1} - C_2 |u|^{\alpha_2} + O(\|\boldsymbol{h}\|^{\alpha_1} + |u|^{\alpha_2})$$

around $(\mathbf{0}, 0)$*, where* $0 < \alpha_1, \alpha_2 \leq 2$ *and* $C_1, C_2 \geq 0$ *are constants independent of* $\boldsymbol{h}$ *and* u*.*

Remark 4.2. The parameters α_1 and α_2 are related to the smoothness of the sample paths in the underlying Gaussian space-time process. For further reference see for example Adler [1], Chapter 2. For a better understanding of the parameters consider the tail dependence coefficient in (3.1), given by $\chi(\boldsymbol{h}, u) = 2(1 - \Phi(\sqrt{C_1 \|\boldsymbol{h}\|^{\alpha_1} + C_2 |u|^{\alpha_2}}))$. For example let $\|\boldsymbol{h}\| = 0$. If α_2 is near zero then $\chi(\mathbf{0}, u)$ is approximately constant indicating that the extremal dependence is the same for all temporal lags $u > 0$. If, in addition, C_2 is large then $\chi(\mathbf{0}, u)$ is close to zero leading to asmyptotic independence. So, the combination of α_2 small and C_2 large leads to asymptotic independence. □

Under Assumption 4.1, the scaling sequences in Assumption 2.1 can be chosen as $s_n = (\log n)^{-1/\alpha_1}$ and $t_n = (\log n)^{-1/\alpha_2}$. It follows that

$$(\log n)(1 - \rho(s_n \boldsymbol{h}, t_n u)) \to C_1 \|\boldsymbol{h}\|^{\alpha_1} + C_2 |u|^{\alpha_2} = \delta(\boldsymbol{h}, u), \; n \to \infty. \quad (4.1)$$

The condition of tightness in (2.3) can be obtained by defining

$$D((\boldsymbol{s}_1, t_1), (\boldsymbol{s}_2, t_2)) = \max \left\{ \|\boldsymbol{s}_1 - \boldsymbol{s}_2\|^{\alpha_1/2}, |t_1 - t_2|^{\alpha_2/2} \right\},$$

which is a metric on $\mathbb{R}^d \times [0, \infty)$, since $\alpha_1, \alpha_2 \in (0, 2]$.

Smith's storm profile model (2.12) can be viewed as a special case of the Brown-Resnick limit process in Theorem 2.2, where the underlying correlation function satisfies Assumption 4.1. In particular, choosing $\alpha_1 = \alpha_2 = 2$ and

$$\sigma_{12} = 0, \; \sigma_1^2 = \sigma_2^2 = \frac{1}{4C_1}, \text{ and } \sigma_3^2 = \frac{1}{4C_2}$$

in the Smith model, we find that $\delta(\boldsymbol{h}, u)$ is of the form given in Assumption 4.1,

$$\delta(\boldsymbol{h}, u) = \frac{1}{4(\sigma_1^2 \sigma_2^2 - \sigma_{12}^2)} (\sigma_2^2 h_1^2 - 2\sigma_{12} h_1 h_2 + \sigma_1^2 h_2^2) + \frac{1}{4\sigma_3^2} u^2,$$

and, hence, has the same finite-dimensional distributions as the Brown-Resnick process.

In the following, we analyse several correlation models used in the literature for modelling Gaussian space-time processes. In recent years, the interest in spatio-temporal correlation models has been growing significantly, especially the construction of valid covariance functions in space and time. A simple way to construct such a model is to take the product of a spatial correlation function $\rho_1(\boldsymbol{h})$ and a temporal correlation function $\rho_2(u)$, i.e. $\rho(\boldsymbol{h}, u) = \rho_1(\boldsymbol{h}) \rho_2(u)$ (see for example Cressie and Huang [10]). Such a model is called separable and Assumption 4.1 is satisfied, if the spatial and the temporal correlation functions have expansions around zero of the form

$$\rho_1(\boldsymbol{h}) = 1 - C_1 \|\boldsymbol{h}\|^{\alpha_1} + o(\|\boldsymbol{h}\|^{\alpha_1}), \quad \rho_2(u) = 1 - C_2 |u|^{\alpha_2} + o(|u|^{\alpha_2}), \quad (4.2)$$

respectively.

A more sophisticated method to obtain separable covariance models is given on a process-based level. An interesting example in this context is presented in Baxevani, Podgórski and Rychlik [3] and Baxevani, Caires and Rychlik [2], who construct Gaussian space-time processes in a continuous setup using moving averages of spatial fields over time, given by

$$X(\boldsymbol{s},t)=\int_{-\infty}^{\infty} f(t-u)\Phi(\boldsymbol{s},du), \tag{4.3}$$

where $\Phi(\cdot,du)$ is a Gaussian spatial field valued measure (see Appendix 5.1 in [2] for a definition) which is uniquely determined by the stationary correlation function $\rho_1(\boldsymbol{h})$ and f is a deterministic kernel function. Note, that the process in (4.3) is a special case of the process introduced in [3].

Consider the kernel function $f(t)=e^{-\lambda t}\mathbb{1}_{\{t\geq 0\}}$ and the stationary spatial covariance model $\rho_1(\boldsymbol{h})=\exp\{-\|\boldsymbol{h}\|^2/C\}$. Using equation (5) in [3], the covariance function for the spatial lag $\boldsymbol{h}$ and the temporal lag $u>0$ can be calculated as

$$\begin{aligned}\gamma(\boldsymbol{h},u)&=\rho_1(\boldsymbol{h})\int_{-\infty}^{\infty} e^{-\lambda(u-y)}\mathbb{1}_{\{u-y\geq 0\}}e^{\lambda y}\mathbb{1}_{\{y\leq 0\}}dy=\rho_1(\boldsymbol{h})\int_{-\infty}^{0} e^{-\lambda u+2\lambda y}dy\\&=\rho_1(\boldsymbol{h})\frac{1}{2\lambda}e^{-\lambda u}=\frac{1}{2\lambda}\exp\left\{-\frac{\|\boldsymbol{h}\|^2}{C}-\lambda u\right\},\end{aligned}$$

where the temporal dependence is of Ornstein-Uhlenbeck type (see Example 2 in [3]). The corresponding correlation function satisfies

$$\rho(\boldsymbol{h},u)=1-\frac{1}{C}\|\boldsymbol{h}\|^2-\lambda|u|+O(\|\boldsymbol{h}\|^2+|u|). \qquad \square$$

Separable space-time models do not allow for any interaction between space and time. Disadvantages of this assumption are pointed out for example in Cressie and Huang [10]. Therefore, nonseparable model constructions have been developed. Another approach for combining purely spatial and temporal covariance functions leading also to nonseparable covariance models is introduced in Ma [30, 31], given in terms of correlation functions by

$$\rho(\boldsymbol{h}, u) = \int_0^\infty \int_0^\infty \rho_1(\boldsymbol{h} v_1)\rho_2(u v_2) dG(v_1, v_2),$$

where G is a bivariate distribution function on $[0, \infty) \times [0, \infty)$. Using the expansions in (4.2), it follows that

$$\rho(\boldsymbol{h}, u) = 1 - C_1 \|\boldsymbol{h}\|^{\alpha_1} \int_0^\infty v_1^{\alpha_1} dG_1(v_1) - C_2 |u|^{\alpha_2} \int_0^\infty v_2^{\alpha_2} dG_2(v_2) + O(\|\boldsymbol{h}\|^{\alpha_1} + |u|^{\alpha_2}),$$

where G_1 and G_2 denote the marginal distribution functions of G, respectively. From this representation, the components in Assumption 4.1 can be read off directly.

4.1. Gneiting's class of correlation functions

A more elaborate class of nonseparable, stationary correlation functions is given by Gneiting's class [24]. This class of covariance functions is based on completely monotone functions, which are defined as functions φ on $(0, \infty)$ with existing derivatives of all orders $\varphi^{(n)}$, $n \geq 0$ and

$$(-1)^n \varphi^{(n)}(t) \geq 0, \quad t > 0,\ n \geq 0.$$

For our purpose we use a slightly different definition of Gneiting's class.

Definition 4.3 (Gneiting's class of correlation functions [24])**.** *Let $\varphi : \mathbb{R}_+ \to \mathbb{R}$ be completely monotone and let $\psi : \mathbb{R}_+ \to \mathbb{R}$ be a positive function with completely monotone derivative. Further assume that $\psi(0)^{-d/2}\varphi(0) = 1$, where d is the spatial dimension, and $\beta_1, \beta_2 \in (0, 1]$. The function*

$$\rho(\boldsymbol{h}, u) = \frac{1}{\psi\left(|u|^{2\beta_2}\right)^{d/2}} \varphi\left(\frac{\|\boldsymbol{h}\|^{2\beta_1}}{\psi\left(|u|^{2\beta_2}\right)}\right), \quad (\boldsymbol{h}, u) \in \mathbb{R}^d \times \mathbb{R}_+, \qquad (4.4)$$

defines a non-separable, isotropic space-time correlation function with $\rho(\mathbf{0}, 0) = 1$.

Compared to the original definition in [24], we included the parameters β_1 and β_2, which is not a restriction since we can simply change the norms by defining $\|\cdot\|_*$ and $|\cdot|_*$ in terms of those in [24] through

$$\|\boldsymbol{h}\|_* = \|\boldsymbol{h}\|^{\beta_1}, \quad \text{and} \quad |u|_* = |u|^{\beta_2}.$$

These new quantities are still norms since $\beta_1, \beta_2 \in (0, 1]$. In the next step, we provide an expansion of the correlation function around zero to guarantee Assumption 4.1. The following proposition generalizes a result of Xue and Xiao [44] (Proposition 6.1).

Proposition 4.4. *Assume that $\psi'(0) \neq 0$. Every correlation function taken from the Gneiting class* (4.4) *satisfies Assumption 4.1 with $\alpha_1 = 2\beta_1$, $\alpha_2 = 2\beta_2$ and*

$$C_1 = \psi(0)^{-1} \left(\int_0^\infty z dF_\varphi(z) \Big/ \int_0^\infty dF_\varphi(z) \right), \quad C_2 = \frac{d}{2}\psi(0)^{-1}\psi'(0), \qquad (4.5)$$

where F_φ is a non-decreasing bounded function with $F_\varphi(0) \neq 0$ and $\int_0^\infty z dF_\varphi(z) < \infty$.

Proof. Since the function φ is completely monotone, Bernstein's theorem (see for example Feller [21], Chapter 13) gives

$$\varphi(x) = \int_0^\infty e^{-xz} dF_\varphi(z), \quad x \geq 0.$$

Since $\psi(0)^{-d/2}\varphi(0) = 1$, it follows that $\psi(0) \neq 0$ and $\varphi(0) \neq 0$. We apply a Taylor expansion to the functions $\psi(\cdot)^{-d/2}$ and the exponential in the representation of φ:

$$\psi(u)^{-d/2} = \psi(0)^{-d/2} - \frac{d}{2}\psi(0)^{-d/2-1}\psi'(0)u + o(u),$$

$$\varphi(x) = \int_0^\infty (1 - xz + o(x)) dF_\varphi(z) = \int_0^\infty dF_\varphi(z) - x \int_0^\infty z dF_\varphi(z) + o(x),$$

for $u \to 0$ and $x \to 0$. Plugging these into (4.4) and replacing u by $|u|^{2\beta_2}$ and x by $\|\boldsymbol{h}\|^{2\beta_1}/\psi(|u|^{2\beta_2})$, we obtain

$$
\begin{aligned}
\rho(\boldsymbol{h}, u) = &\left(\psi(0)^{-d/2} - \frac{d}{2}\psi(0)^{-d/2-1}\psi'(0)|u|^{2\beta_2} + o(|u|^{2\beta_2})\right) \\
&\times \Bigg(\int_0^\infty dF_\varphi(z) - \int_0^\infty z dF_\varphi(z)\|\boldsymbol{h}\|^{2\beta_1}\left[\psi(0)^{-1} - \psi(0)^{-2}\psi'(0)|u|^{2\beta_2}\right. \\
&\quad \left. + o(|u|^{2\beta_2})\right] + o(\|\boldsymbol{h}\|^{2\beta_1})\Bigg) \\
= &\ \psi(0)^{-d/2}\varphi(0) - \frac{d}{2}\psi(0)^{-d/2-1}\varphi(0)\psi'(0)|u|^{2\beta_2} - \psi(0)^{-d/2-1}\int_0^\infty z dF_\varphi(z)\|\boldsymbol{h}\|^{2\beta_1} \\
&+ O(\|\boldsymbol{h}\|^{2\beta_1} + |u|^{2\beta_2}) \\
= &\ 1 - \frac{d}{2}\psi(0)^{-1}\psi'(0)|u|^{2\beta_2} - \psi(0)^{-1}\left(\int_0^\infty z dF_\varphi(z) \Big/ \int_0^\infty dF_\varphi(z)\right)\|\boldsymbol{h}\|^{2\beta_1} \\
&+ O(\|\boldsymbol{h}\|^{2\beta_1} + |u|^{2\beta_2}) \\
= &\ 1 - C_1\|\boldsymbol{h}\|^{2\beta_1} - C_2|u|^{2\beta_2} + O(\|\boldsymbol{h}\|^{2\beta_1} + |u|^{2\beta_2}),
\end{aligned}
$$

where C_1 and C_2 are defined as in (4.5). □

Remark 4.5. For various choices of $\alpha_1, \alpha_2 \in (0, 2]$, the correlation functions in the Gneiting class have the flexibility to model different levels of smoothness of the underlying Gaussian process.

Example 4.6. We illustrate Gneiting's class (4.4) by a specific example, where the functions ϕ and ψ are taken from [24]; namely

$$\varphi(x) = (1 + bx)^{-\nu}, \quad \psi(x) = (1 + ax)^{\gamma}, \ x > 0,$$

where $a, b, \nu > 0$ and $0 < \gamma \leq 1$. The function φ is the Laplace transform of a gamma density with shape parameter $\nu > 0$ and scale parameter $b > 0$, which has mean $b\nu$. The first-order derivative of ψ at zero is given by $\psi'(0) = a\gamma$.

We choose $\beta_1 = \beta_2 = 1$ leading to $\alpha_1 = \alpha_2 = 2$ and, thus, a mean-square differentiable Gaussian process. The constants C_1 and C_2 are given by

$$C_1 = b\nu, \quad \text{and } C_2 = \frac{d}{2} a\gamma.$$

Figure 1 shows contour plots of the correlation function and the resulting tail dependence coefficient as in (3.1) based on different values for a and b with $\nu = 3/2$ and $\gamma = 1$ fixed as a function of the space-lag $\|\boldsymbol{h}\|$ and time lag $|u|$. We see that the tail dependence function exhibits virtually the identical pattern of the underlying correlation function under a compression of the space-time scale. In particular, the extremal dependence dies out more quickly for large space and time lags than for the correlation function.

In a second step, we simulate space-time processes using the above defined correlation model with $a = b = 0.03$, $\nu = 3/2$ and $\gamma = 1$. We start the simulation procedure with $n = 100$ replications of a Gaussian process with correlation function $\rho(s_n \boldsymbol{s}, t_n u)$ using the simulation routine in the R-package `RandomFields` by Schlather [38]. The space-time processes are then transformed to standard Fréchet and the pointwise maximum is taken over the 100 replications. Figure 2 shows image and contour plots (using the R-package `fields` for visualization) of the simulated processes for four consecutive time points and different marginal distributions. The first column in Figure 2 shows the max-stable processes with standard Fréchet marginal distributions, whereas the second and third column show the resulting processes, if the margins are transformed to standard Gumbel and Weibull, respectively. Clearly, in the last two models the peaks are not as high and pronounced as in the Fréchet model. One still sees the separated peaks in the Fréchet case, which are well-known from the Smith's storm profile model when using a centered Gaussian density for the function f.

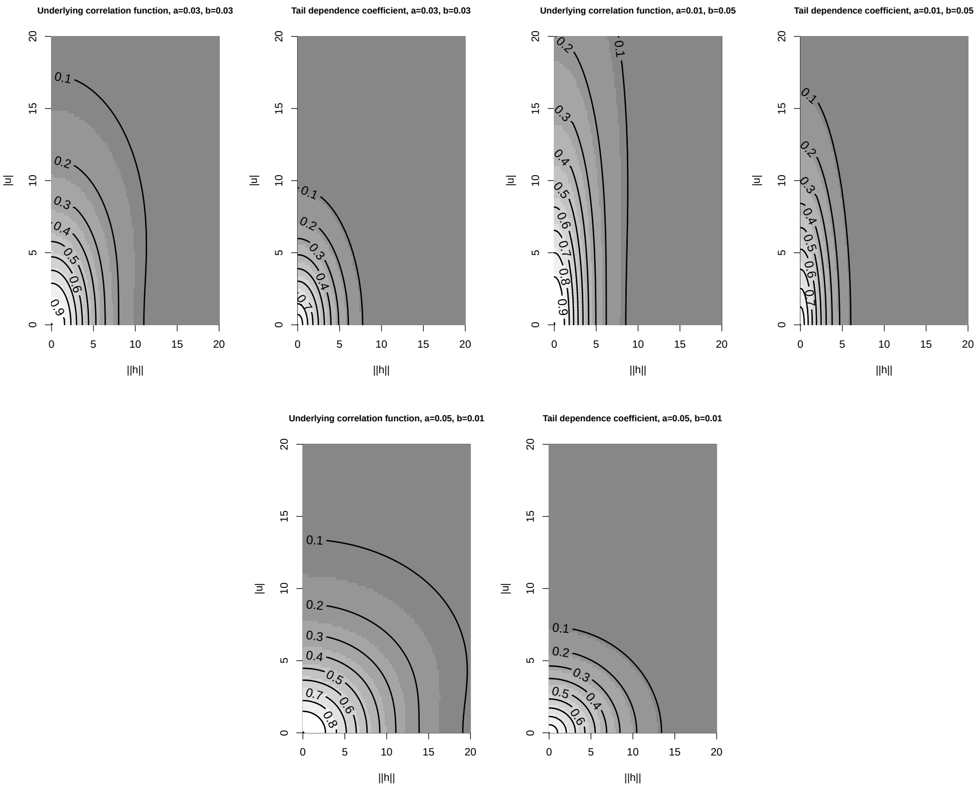

Figure 1: Contour plots for the underlying correlation function (left) and the resulting tail dependence coefficient function (right) depending on the absolute space lag $\|\boldsymbol{h}\|$ and time lag $|u|$ for different values of the scaling parameters a (time) and b (space), $\nu = 3/2$ and $\gamma = 1$.

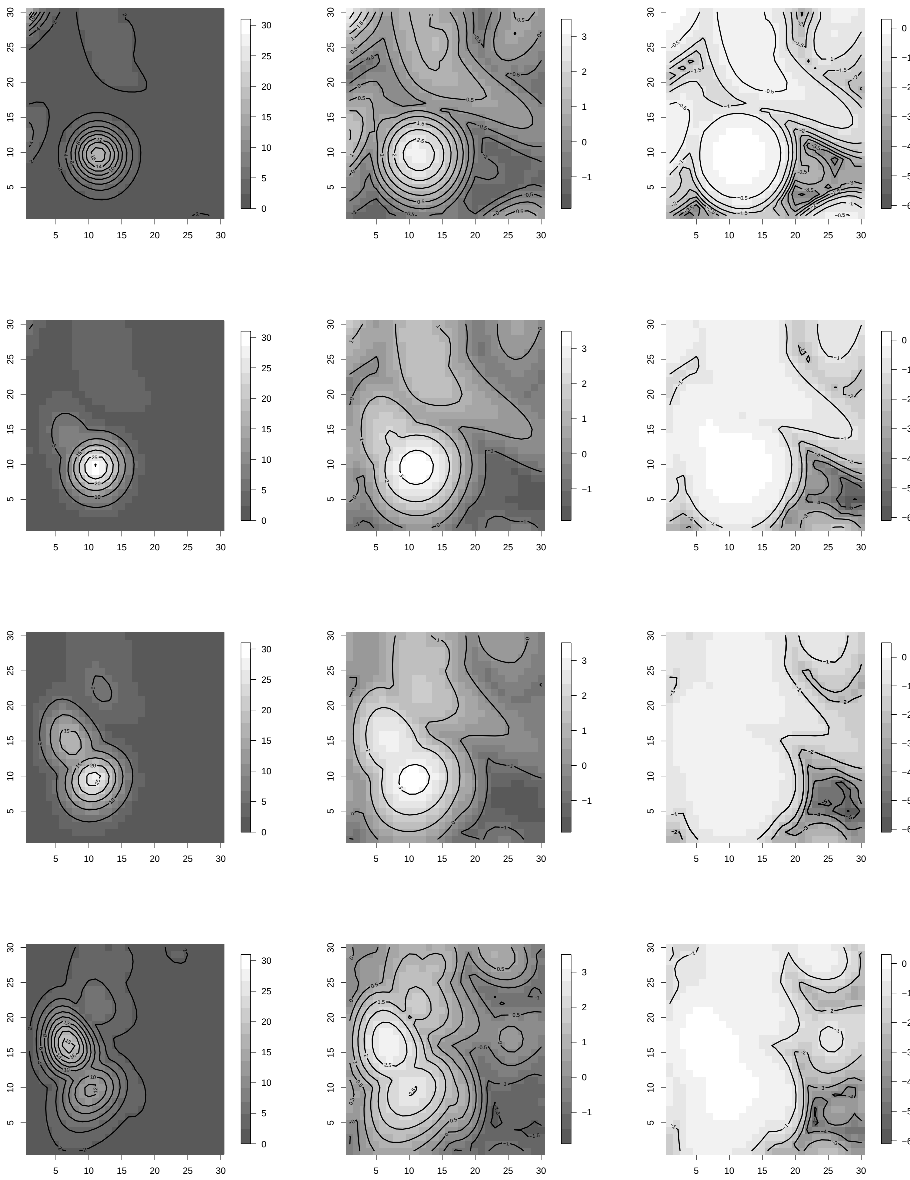

Figure 2: Simulated max-stable processes with Fréchet (left), Gumbel (middle) and Weibull (right) marginal distributions ($a = 0.03, b = 0.03, \nu = -3/2,\ \gamma = 1$) for four consecutive time points (from top to bottom) with time lag one using a grid simulation of size 30×30.

4.2. Modelling spatial anisotropy

The correlation functions of the underlying Gaussian spatial fields in the previous sections were spatially isotropic, meaning that the correlation functions only depend on the absolute space and time lags $\|\boldsymbol{h}\|$ and $|u|$. An easy way to introduce spatial anisotropy to a model is by geometric anisotropy, i.e.,

$$\tilde{\rho}(\boldsymbol{h}, u) = \rho(\|A\boldsymbol{h}\|, |u|),$$

where A is a transformation matrix. In the bivariate case geometric anisotropy in space can be modelled by a transformation matrix $A = TR$, with rotation matrix R and distance matrix T, where

$$R = \begin{pmatrix} \cos\alpha & -\sin\alpha \\ \sin\alpha & \cos\alpha \end{pmatrix}, \quad T = \begin{pmatrix} 1/a_{\max} & 0 \\ 0 & 1/a_{\min} \end{pmatrix}. \tag{4.6}$$

Geometric anisotropy directly relates to the tail dependence coefficient yielding

$$\chi(\boldsymbol{h}, u) = 2(1 - \Phi(\sqrt{\delta(A\boldsymbol{h}, u)})).$$

Figure 3 compares isotropic and anisotropic correlation functions and the corresponding tail dependence coefficients as function of the space lag components $\boldsymbol{h} = (h_1, h_2)'$, where the isotropic correlation is the same as in Example 4.6 with $\gamma = 1$, $\nu = 3/2$ and $a = b = 0.03$. For the anisotropic case we choose $a_{\min} = 1$, $a_{\max} = 3$ and $\alpha = 45°$. It can be seen, that the structure in the correlation function translates to the tail dependence coefficient. Corresponding max-stable processes with Fréchet margins are shown for four consecutive time points in Figure 4. From the image plots, one clearly sees that the correlation is stronger in one direction. The perspective plots show that the isolated peaks are now no longer spherical, but elliptical. In reality, this could correspond to wind speed peaks coming for example from a storm shaped particular in this wind direction.

A more complex way of introducing anisotropy in space is given by the Bernstein class, which is introduced in Porcu et al. [36] and revisited in Mateu et al. [33]. The covariance model is defined by

$$C(\boldsymbol{h}, u) = \int_0^\infty\int_0^\infty \exp\left\{-\sum_{i=1}^{d}\psi_i(|h_i|)v_1 - \psi^{(t)}(|u|)v_2\right\} dF(v_1, v_2),$$

where F is a bivariate distribution function and $\psi_i, i = 1, \ldots, d$ and $\psi^{(t)}$ are positive functions on $[0, \infty)$ with completely monotone derivatives, also called Bernstein functions. We assume that $\psi_i, i = 1, \ldots, d$ and $\psi^{(t)}$ are standardized, such that $\psi_i(0) = \psi_t(0) = 1, i = 1, \ldots, d$. Assumption 2.1 can directly be derived for the corresponding correlation function. Note, that the following "=" are not exact due to approximations made in the calculations.

$$\begin{aligned}
&\rho(\boldsymbol{h}, u) = C(\boldsymbol{h}, u)/C(\mathbf{0}, 0) \\
&= \left(1 - \sum_{i=1}^{d}\psi_i(|h_i|)\int_0^\infty\int_0^\infty v_1 dF(v_1, v_2) - \psi^{(t)}(|u|)\int_0^\infty\int_0^\infty v_2 dF(v_1, v_2)\right)\Big/ \\
&\quad \left(1 - d\int_0^\infty\int_0^\infty v_1 dF(v_1, v_2) - \int_0^\infty\int_0^\infty v_2 dF(v_1, v_2)\right) \\
&= \left(1 - \sum_{i=1}^{d}(1 - C_1|h_i|^{\alpha_1})\int_0^\infty v_1 F_{v_1}(v_1) - (1 - C_2|u|^{\alpha_2})\int_0^\infty v_2 dF_{v_2}(v_2)\right)\Big/ \\
&\quad \left(1 - d\int_0^\infty v_1 dF_{v_1}(v_1) - \int_0^\infty v_2 dF_{v_2}(v_2)\right) + o(\sum_{i=1}^{d}|h_i|^{\alpha_1}) + o(|u|^{\alpha_2}) \\
&= 1 - C_1\int_0^\infty v_1 dF_{v_1}(v_1)\sum_{i=1}^{d}|h_i|^{\alpha_1} - C_2\int_0^\infty v_2 dF_{v_2}(v_2)|u|^{\alpha_2} \\
&\quad + O(\sum_{i=1}^{d}|h_i|^{\alpha_1} + |u|^{\alpha_2})
\end{aligned}$$

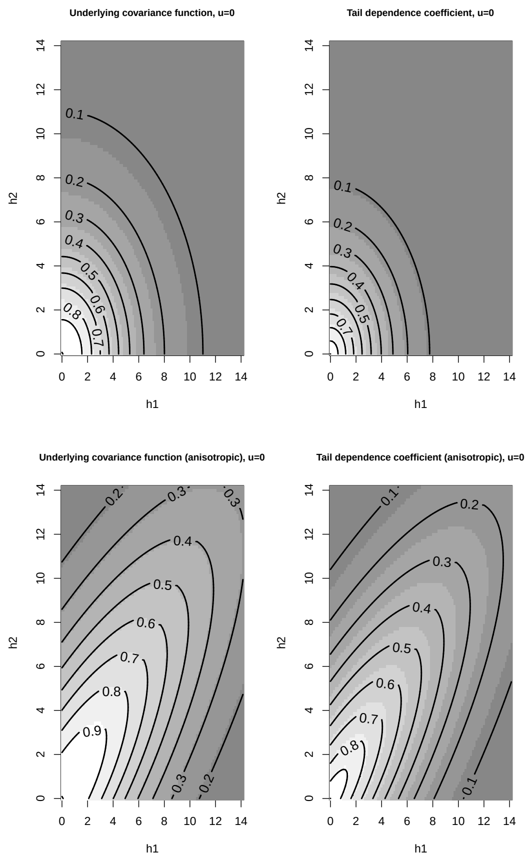

Figure 3: Contour plots for covariance and tail dependence functions depending on the space lag components h_1 and h_2 in the isotropic case (left) and for the geometric anisotropy model (right), where we have chosen $a = b = 0.03$, $a_{\min} = 1$, $a_{\max} = 3$ and $\alpha = 45°$ in (4.6).

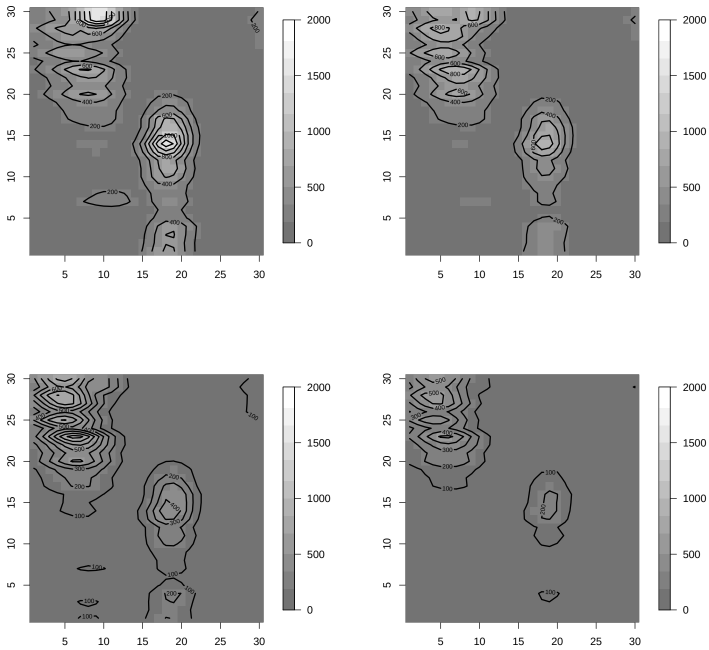

Figure 4: Simulated anisotropic max-stable processes with Fréchet marginal distributions with anisotropic parameters $a_{\min} = 1$, $a_{\max} = 3$ and $\alpha = 45°$ in (4.6) for four consecutive time points (from top left to bottom right).

5. Conlusion

The main objective of this paper was to extend concepts of max-stable spatial fields to the space-time domain. We extended the construction of max-stable spatial fields as pointwise limits of rescaled and transformed Gaussian spatial fields (see Brown and Resnick [] and Kabluchko et al. [27]) In a second step, we extended Smith's storm profile model [42]. For both max-stable space-time processes we calculated the resulting bivariate distribution functions, which are equal under certain parameter restrictions.

We showed that the limit assumption on the correlation function in the underlying Gaussian process relates to the tail dependence function in the max-stable process. Several examples of spatio-temporal correlation functions and their connection to the tail dependence function have been presented. We extended an assumption on the correlation model known from the analysis of extremes of stationary Gaussian processes (see Leadbetter et al. [29]) and showed how Gneiting's class of covariance functions [24] fits in this context. Visualizations of our results were shown in form of contour plots of the underlying correlation functions and the corresponding tail dependence functions. In addition, we simulated max-stable space-time processes using different marginal distributions and an anisotropic correlation function. In particular, geometric anisotropy in the underlying correlation function leads to directional movements in Smith's storm profile model.

In Davis, Klüppelberg and Steinkohl [12], composite likelihood methods for the estimation of the max-stable space-time processes introduced in this paper, are investigated. In particular, pairwise likelihood methods based on the bivariate distribution function in (2.6) are used to estimate the location and scale parameters. For M observation locations $\boldsymbol{s}_1, \ldots, \boldsymbol{s}_M$ and T time points $t_1, \ldots, t_T$ the pairwise log-likelihood is given by

$$PL^{(M,T)}(\boldsymbol{\psi}) = \sum_{i=1}^{M-1} \sum_{j=i+1}^{M} \sum_{k=1}^{T-1} \sum_{l=k+1}^{T} \log f_{(C_1,\alpha_1,C_2,\alpha_2)}(\eta(\boldsymbol{s_i}, t_k), \eta(\boldsymbol{s}_j, t_l)),$$

where $f_{(C_1,\alpha_1,C_2,\alpha_2)}(x_1, x_2)$ is the bivariate density of the max-stable process. $PL^{(M,T)}$ is maximized to obtain estimates for C_1, α_1, C_2 and α_2. It turns out that the estimates are strongly consistent and asymptotically normal. For more information regarding accuracy of the estimates we refer to Davis et al. [12]. Another estimation method is based on an empirical version of the tail dependence function (the extremogram) in (3.1), which can be used to estimate the parameters using weighted linear regression methods; cf. Davis et al. [11] for details and an application to radar rainfall data.

Acknowledgments

All authors gratefully acknowledge the support by the TUM Institute for Advanced Study (TUM-IAS). The third author additionally likes to thank the International Graduate School of Science and Engineering (IGSSE) of the

Technische Universität München for their support. The research of Richard A. Davis was also supported in part by the National Science Foundation grant DMS-1107031.

References

[1] R.J. Adler. *The Geometry of Random Fields*. John Wiley, New York, 1981.

[2] A. Baxevani, S. Caires, and I. Rychlik. Spatio-temporal stationary modelling of significant wave height. *Environmetics*, 20(1):14–31, 2009.

[3] A. Baxevani, K. Podgórski, and I. Rychlik. Dynamically evolving Gaussian spatial random fields. *Extremes*, 14(2):223–251, 2011.

[4] J. Beirlant, Y. Goegebeur, J. Segers, and J. Teugels. *Statistics of Extremes, Theory and Applications*. Wiley Series in Probability and Statistics, John Wiley & Sons Ltd, Chichester, 2004.

[5] B.M. Brown and S.I. Resnick. Extreme values of independent stochastic processes. *Journal of Applied Probability*, 14(4):732–739, 1977.

[6] S.G. Coles. Regional modelling of extreme storms via max-stable processes. *Journal of the Royal Statistical Society B*, 55(4):797–816, 1993.

[7] S.G. Coles. *An Introduction to Statistical Modeling of Extreme Values*. Springer Series in Statistics, Springer, New York, 2001.

[8] S.G. Coles and J.A Tawn. Modelling extremes of the areal rainfall process. *Journal of the Royal Statistical Society B*, 58(2):329–347, 1996.

[9] S.G. Coles and D. Walshaw. Directional modelling of extreme wind speeds. *Journal of the Royal Statistical Society C*, 43:139–157, 1994.

[10] N. Cressie and H.C. Huang. Classes of nonseperable spatio-temporal stationary covariance functions. *Journal of the American Statistical Association*, 94(448):1330–1340, 1999.

[11] R.A. Davis, C. Klüppelberg, and C. Steinkohl. A semiparametric estimation procedure for max-stable space-time processes. 2012. In preparation.

[12] R.A. Davis, C. Klüppelberg, and C. Steinkohl. Statistical inference for max-stable processes in space and time. *Journal of the Royal Statistical Society B*, 2012. to appear.

[13] R.A. Davis and T. Mikosch. Extreme value theory for space-time processes with heavy-tailed distributions. *Stochastic Processes and their Applications*, 118(4):560–584, 2008.

[14] R.A. Davis and T. Mikosch. The extremogram: A correlogram for extreme events. *Bernoulli*, 15(4):977–1009, 2009.

[15] L. de Haan. A spectral representation for max-stable processes. *The Annals of Probability*, 12(4):1194–1204, 1984.

[16] L. de Haan and A. Ferreira. *Extreme Value Theory: An Introduction.* Springer Series in Operations Research and Financial Engineering, New York, 2006.

[17] L. de Haan and J. Pickands. Stationary min-stable stochastic processes. *Probability Theory and Related Fields*, 72(4):477–492, 1986.

[18] P. Deheuvels. Point processes and multivariate extreme values. *Journal of Multivariate Analysis*, 13(2):257–272, 1983.

[19] P. Embrechts, C. Klüppelberg, and T. Mikosch. *Modelling Extremal Events.* Springer, Berlin, 1997.

[20] V. Fasen, C. Klüppelberg, and M. Schlather. High-level dependence in time series models. *Extremes*, 13(1):1–33, 2010.

[21] W. Feller. *An introduction to probability theory and its applications*, volume 2 of *Wiley series in probability and mathematical statistics: Probability and mathematical statistics.* Wiley, 1971.

[22] J. Geffroy. Contributions à la théorie des valeurs extrème. *Publ. Inst. Stat. Univ. Paris*, 7:36–123, 1958.

[23] J. Geffroy. Contributions à la théorie des valeurs extrème. *Publ. Inst. Stat. Univ. Paris*, 8:3–52, 1959.

[24] T. Gneiting. Nonseparable, stationary covariance functions for space-time data. *Journal of the American Statistical Association*, 95(458):590–600, 2002.

[25] J. Hüsler and R.-D. Reiss. Maxima of normal random vectors: between independence and complete dependence. *Statistics and Probability Letters*, 7(4):283–286, 1989.

[26] Z. Kabluchko. Extremes of space-time Gaussian processes. *Stochastic Processes and their Applications*, 119:3962–3980, 2009.

[27] Z. Kabluchko, M. Schlather, and L. de Haan. Stationary max-stable fields associated to negative definite functions. *The Annals of Probability*, 37(5):2042–2065, 2009.

[28] M.R. Leadbetter. On extreme values in stationary sequences. *Zeitschrift für Wahrscheinlichkeitstheorie und verwandte Gebiete*, 28:289–303, 1974.

[29] M.R. Leadbetter, G. Lindgren, and H. Rootzén. *Extremes and Related Properties of Random Sequences and Processes*. Springer Verlag, New York, 1983.

[30] C. Ma. Spatio-temporal covariance functions generated by mixtures. *Mathematical geology*, 34(8):965–975, 2002.

[31] C. Ma. Spatio-temporal stationary covariance functions. *Journal of Multivariate Analysis*, 86(1):97–107, 2003.

[32] C. Ma. Linear combinations of space-time covariance functions and variograms. *IEEE Transactions on signal processing*, 53(3):857–864, 2005.

[33] J. Mateu, E. Porcu, and P. Gregori. Recent advances to model anisotropic space-time data. *Statistical Methods and Applications*, 17(2):209–223, 2007.

[34] S.A. Padoan, M. Ribatet, and S.A. Sisson. Likelihood-based inference for max-stable processes. *Journal of the American Statistical Association*, 105(489):263–277, 2009.

[35] J. Pickands. Multivariate extreme value distributions. *Proceedings of the 43rd Session of the Int. Stat. Institute*, pages 859–878, 1981.

[36] E. Porcu, P. Gregori, and J. Mateu. La descente et la montée étendues: the spatially d-anisotropic and spatio-temporal case. *Stochastic Environmental Research and Risk Assessment*, 21(6):683–693, 2007.

[37] H. Sang and A. Gelfand. Hierarchical modeling for extreme values observed over space and time. *Environmental and Ecological Statistics*, 16(3):407–426, 2009.

[38] M. Schlather. Models for stationary max-stable random fields. *Extremes*, 5(1):33–44, 2002.

[39] M. Schlather. Some covariance models based on normal scale mixtures. *Bernoulli*, 16(3):780–797, 2010.

[40] M. Schlather and J.A. Tawn. A dependence measure for multivariate and spatial extreme values: Properties and inference. *Biometrika*, 90(1):139–156, 2003.

[41] M. Sibuya. Bivariate extreme statistics. *Annals of the Institute of Statistical Mathematics*, 11:195–210, 1960.

[42] R. L. Smith. Max-stable processes and spatial extremes. Unpublished manuscript, University of North California, 1990.

[43] H. Wackernagel. *Multivariate Geostatistics*. Springer, Heidelberg, 2003.

[44] Y. Xue and Y. Xiao. Fractal and smoothness properties of space-time gaussian models. *Frontiers of Mathematics in China*, 6(6):1217–1248, 2011.

Appendix A. Derivation of the bivariate distribution function for the Smith space-time process

Proof. (Theorem 2.6) Since space and time are independent, we can write

$$f_0(\boldsymbol{z}, x) = f_1(\boldsymbol{z}) f_2(x), \quad \boldsymbol{z} \in \mathbb{R}^2,\ x \in \mathbb{R}$$

where f_1 is the density of a bivariate normal distribution with mean $\mathbf{0}$ and covariance matrix Σ, and f_2 is the density of a normal distribution with mean 0 and variance σ_3^2. Starting from equation (2.13) with $K = 2$, we obtain

$$\begin{aligned}
&F(y_1, y_2)\\
&= \exp\left\{ -\int_{-\infty}^{\infty}\int_{-\infty}^{\infty}\int_{-\infty}^{\infty} \left(\frac{f_0(\boldsymbol{z}, x)}{y_1}\right) \vee \left(\frac{f_0(\boldsymbol{z}-\boldsymbol{h}, x-u)}{y_2}\right) d\boldsymbol{z}dx \right\}\\
&= \exp\left\{ -\int_{-\infty}^{\infty}\int_{-\infty}^{\infty}\int_{-\infty}^{\infty} \frac{f_0(\boldsymbol{z}, x)}{y_1} \mathbb{1}\left\{\frac{f_0(\boldsymbol{z}, x)}{y_1} \geq \frac{f_0(\boldsymbol{z}-\boldsymbol{h}, x-u)}{y_2}\right\} d\boldsymbol{z}dx \right.\\
&\quad \left. -\int_{-\infty}^{\infty}\int_{-\infty}^{\infty}\int_{-\infty}^{\infty} \frac{f_0(\boldsymbol{z}-\boldsymbol{h}, x-u)}{y_2} \mathbb{1}\left\{\frac{f_0(\boldsymbol{z}-\boldsymbol{h}, x-u)}{y_2} \geq \frac{f_0(\boldsymbol{z}, x)}{y_1}\right\} d\boldsymbol{z}dx \right\}\\
&= \exp\{-(\mathrm{I}) - (\mathrm{II})\}
\end{aligned}$$

$$
\begin{aligned}
(\mathrm{I}) &= \int_{-\infty}^{\infty} f_2(x) \int_{-\infty}^{\infty}\int_{-\infty}^{\infty} \frac{f_1(\boldsymbol{z})}{y_1} \mathbb{1}\left\{ \frac{f_1(\boldsymbol{z}) f_2(x)}{y_1} \geq \frac{f_1(\boldsymbol{z}-\boldsymbol{h}) f_2(x-u)}{y_2} \right\} d\boldsymbol{z} dx \\
&= \int_{-\infty}^{\infty} f_2(x) \frac{1}{y_1} \mathbb{E}\left[\mathbb{1}\left\{ \frac{f_1(\boldsymbol{Z}) f_2(x)}{y_1} \geq \frac{f_1(\boldsymbol{Z}-\boldsymbol{h}) f_2(x-u)}{y_2} \right\} \right] dx,
\end{aligned}
$$

where $\boldsymbol{Z}$ has a normal density with mean $\mathbf{0}$ and variance Σ. Now note that

$$
\begin{aligned}
&\frac{f_1(\boldsymbol{Z}) f_2(x)}{y_1} \geq \frac{f_1(\boldsymbol{Z}-\boldsymbol{h}) f_2(x-u)}{y_2} \Leftrightarrow f_1(\boldsymbol{Z}) \geq f_1(\boldsymbol{Z}-\boldsymbol{h}) \frac{y_1}{y_2} \frac{f_2(x-u)}{f_2(x)} \\
&\Leftrightarrow (2\pi)^{-d/2} |\Sigma|^{-1} \exp\left\{ -\frac{1}{2} \boldsymbol{Z}^T \Sigma^{-1} \boldsymbol{Z} \right\} \\
&\qquad \geq (2\pi)^{-d/2} |\Sigma|^{-1} \exp\left\{ -\frac{1}{2} (\boldsymbol{Z}-\boldsymbol{h})^T \Sigma^{-1} (\boldsymbol{Z}-\boldsymbol{h}) \right\} \frac{y_1}{y_2} \frac{f_2(x-u)}{f_2(x)} \\
&\Leftrightarrow \boldsymbol{Z}^T \Sigma^{-1} \boldsymbol{Z} \\
&\qquad < \boldsymbol{Z}^T \Sigma^{-1} \boldsymbol{Z} - 2\boldsymbol{Z}^T \Sigma^{-1} \boldsymbol{h} + \boldsymbol{h}^T \Sigma^{-1} \boldsymbol{h} - 2\log\left(\frac{y_1}{y_2}\right) - 2\log\left(\frac{f_2(x-u)}{f_2(x)}\right) \\
&\Leftrightarrow \boldsymbol{Z}^T \Sigma^{-1} \boldsymbol{h} \leq \frac{1}{2} \boldsymbol{h}^T \Sigma^{-1} \boldsymbol{h} - \log\left(\frac{y_1}{y_2}\right) - \log\left(\frac{f_2(x-u)}{f_2(x)}\right).
\end{aligned}
$$

The random variable $\boldsymbol{Z}^T \Sigma^{-1} \boldsymbol{h} =: \boldsymbol{Z}^T B$ is normally distributed with mean $\mathbf{0}$ and variance

$$
B^T \Sigma B = \boldsymbol{h}^T \Sigma^{-1} \Sigma \Sigma^{-1} \boldsymbol{h} = \boldsymbol{h}^T \Sigma^{-1} \boldsymbol{h}.
$$

Since f_2 is the density of a zero mean normal distribution with variance σ_3^2, we obtain

$$
\log\left(\frac{f_2(x-u)}{f_2(x)}\right) = -\frac{1}{2\sigma_3^2}(u^2 - 2ux).
$$

With $a(\boldsymbol{h}) = (\boldsymbol{h}^T\Sigma^{-1}\boldsymbol{h})^{1/2}$ and $\boldsymbol{Z}^T\Sigma^{-1}\boldsymbol{h}/a(\boldsymbol{h}) \sim \mathcal{N}(0,1)$ it follows that

$$
\begin{aligned}
&P\left(\boldsymbol{Z}^T\Sigma^{-1}\boldsymbol{h} \leq \frac{1}{2}\boldsymbol{h}^T\Sigma^{-1}\boldsymbol{h}^T - \log\left(\frac{y_1}{y_2}\right) - \log\left(\frac{f_2(x-u)}{f_2(x)}\right)\right) \\
&= P\left(\frac{\boldsymbol{Z}^T\Sigma^{-1}\boldsymbol{h}}{a(\boldsymbol{h})} \leq \frac{a(\boldsymbol{h})}{2} - \frac{\log(y_1/y_2)}{a(\boldsymbol{h})} + \frac{1}{2\sigma_3^2 a(\boldsymbol{h})}(u^2 - 2ux)\right) \\
&= \Phi\left(\frac{a(\boldsymbol{h})}{2} + \frac{\log(y_2/y_1)}{a(\boldsymbol{h})} + \frac{u^2 - 2ux}{2\sigma_3^2 a(\boldsymbol{h})}\right).
\end{aligned}
$$

Altogether, for independent random variables N and X with N standard normally distributed and X normally distributed with mean 0 and variance σ_3^2, we calculate

$$
\begin{aligned}
(\mathrm{I}) &= \frac{1}{y_1}\int_{-\infty}^{\infty} f_2(x)\Phi\left(\frac{a(\boldsymbol{h})}{2} + \frac{\log(y_2/y_1)}{a(\boldsymbol{h})} + \frac{u^2}{2\sigma_3^2 a(\boldsymbol{h})} - \frac{u}{\sigma_3^2 a(\boldsymbol{h})}x\right) dx \\
&= \frac{1}{y_1}P\left(N + \frac{u}{\sigma_3 a(\boldsymbol{h})}\frac{X}{\sigma_3} \leq \frac{a(\boldsymbol{h})}{2} + \frac{\log(y_2/y_1)}{a(\boldsymbol{h})} + \frac{u^2}{2\sigma_3^2 a(\boldsymbol{h})}\right) \\
&= \frac{1}{y_1}\Phi\left(\frac{\frac{a(\boldsymbol{h})}{2} + \frac{\log(y_2/y_1)}{a(\boldsymbol{h})} + \frac{u^2}{2\sigma_3^2 a(\boldsymbol{h})}}{\sqrt{1 + \frac{u^2}{\sigma_3^2 a(\boldsymbol{h})^2}}}\right) \\
&= \frac{1}{y_1}\Phi\left(\frac{2\sigma_3^2\log(y_2/y_1) + \sigma_3^2 a(\boldsymbol{h})^2 + u^2}{2\sigma_3\sqrt{\sigma_3^2 a(\boldsymbol{h})^2 + u^2}}\right),
\end{aligned}
$$

since $N + u/(\sigma_3 a(\boldsymbol{h}))(X/\sigma_3)$ is normally distributed with mean 0 and variance $1 + u^2/(\sigma_3^2 a(\boldsymbol{h})^2)$.
Analogously to (I), using the substitution $\boldsymbol{Z} \to \boldsymbol{Z} + \boldsymbol{h}$, we obtain the second term (II) in (2.16). □